Sm-activated barium halide nanocrystals in fluorozirconate glasses

2008 J. Phys.: Condens. Matter 20 295227

(http://iopscience.iop.org/0953-8984/20/29/295227)

J. Phys.: Condens. Matter **20** (2008) 295227 (4pp) doi:10.1088/0953-8984/20/29/295227

Sm-activated barium halide nanocrystals in fluorozirconate glasses

B Ahrens[1], J Selling[1], C Eisenschmidt[2], A Engel[3] and S Schweizer[4,5,6]

[1] Department of Physics, Faculty of Science, University of Paderborn, Warburger Straße 100, D-33098 Paderborn, Germany
[2] Institute of Physics, Martin-Luther-University of Halle-Wittenberg, Hoher Weg 8, D-06120 Halle (Saale), Germany
[3] Corporate Research and Technology Development, Schott AG, D-55125 Mainz, Germany
[4] Fraunhofer Center for Silicon Photovoltaics, Walter-Hülse-Straße 1, D-06120 Halle (Saale), Germany
[5] Institute of Physics, Martin-Luther-University of Halle-Wittenberg, Heinrich-Damerow-Straße 4, D-06120 Halle (Saale), Germany

E-mail: Stefan.Schweizer@csp.fraunhofer.de

Received 9 January 2008, in final form 14 June 2008
Published 1 July 2008
Online at stacks.iop.org/JPhysCM/20/295227

Abstract
Fluorozirconate-based glasses have been doped with samarium and bromine ions. Thermal processing initiates the formation of barium bromide nanocrystals in the glass. Samarium enters the glass matrix either in its divalent or in its trivalent state. Fluorescence measurements indicate that during the annealing process Sm^{2+} ions enter the nanocrystals leading to enhanced fluorescence efficiency and to changes in the fluorescence lifetime.

1. Introduction

Fluorozirconate (FZ) glasses are characterized by low-phonon energies, a critical parameter leading to reduced non-radiative losses and increased fluorescence efficiencies from rare-earth (RE) ion doping. For example, in digital radiography, FZ glasses have been doped with europium and chlorine ions resulting in very efficient glass-ceramic radiation detectors [1, 2] where the RE ion, europium, is incorporated into the glass as well as in the barium chloride nanocrystals formed in the glass upon annealing.

FZ-based glass ceramics offer a broad range of applications; the functionality can be modified not only by appropriate thermal processing but also by appropriate rare-earth doping. In this work we describe our investigations on Sm-doped fluorobromozirconate (FBZ) glass ceramics. Fluorescence from samarium in FZ glasses has attracted much attention in the past two decades; in particular for studies on spectral-hole burning, excited state absorption, and laser properties.

[6] Author to whom any correspondence should be addressed.

2. Experimental details

2.1. Samples

The Sm-doped FBZ glass ceramics are based on the well-known ZBLAN composition [3]; they are composed of $52ZrF_4$–$20BaF_2$–$15NaBr$–$5NaF$–$3AlF_3$–$1.5LaF_3$–$1.5YF_3$–$1InF_3$–$1SmBr_2$, where values are in molar%. The constituent chemicals were melted in a glassy carbon crucible at 745 °C in an inert atmosphere of nitrogen and then poured into a brass mold that was at a temperature of 200 °C, i.e. below the glass transition temperature of 260 °C for an FZ-based glass [3], before being slowly cooled to room temperature. Additional subsequent annealing steps were also performed in the inert nitrogen atmosphere.

Several sets of Sm-doped FBZ glass ceramics were made. The visible appearance of the as-made FBZ glasses is either transparent dark reddish-brown or clear-colorless. Fluorescence measurements showed that the reddish-brown colored FBZ glasses contain Sm in its divalent state while in the clear glasses the Sm^{2+} dopant was completely converted to Sm^{3+}; we assume that oxygen impurities in the raw materials is the reason for that. Some samples contain both kinds of ions.

After thermal processing of the FBZ glasses containing Sm^{2+}, there is evidence of crystallization from the appearance of the glass, which ranges from clear dark reddish-brown to one which is opaque and slightly milky. The FBZ glasses containing only Sm^{3+} were not thermally processed. All glass samples were cut into 8 mm × 6 mm × 1 mm plates and polished.

2.2. Setup

Fluorescence and fluorescence excitation spectra were recorded using a single-beam spectrometer in which two 0.22 m double monochromators were available for excitation and emission. The excitation was carried out with a halogen or a xenon lamp and the fluorescence was detected with a cooled photomultiplier using single photon counting. The spectra were not corrected for spectral sensitivity of the experimental setup.

For the time-resolved fluorescence measurements a xenon lamp/0.22 m monochromator/chopper combination was used for excitation; the fluorescence signal was detected with the photomultiplier and recorded with a digital oscilloscope.

The x-ray diffraction (XRD) investigations were performed with a commercial x-ray diffractometer (Siemens D5000) operating at 40 kV and 30 mA in the Bragg–Brentano geometry with a monochromator.

3. Experimental results

3.1. X-ray diffraction

The XRD data of FBZ glass ceramics containing Sm^{2+} ions are comprised of very broad peaks at about 26° and 47°, typical for glasses close to the ZBLAN formulation for copper $K\alpha_1$ radiation. In addition, relatively sharp peaks are superimposed on the broad glass background; these peaks grow upon annealing for 20 min at temperatures between 260 and 290 °C. Figure 1(a) shows the XRD data for the as-made, the 270, and the 290 °C sample. We identify the sharp peaks as reflections from hexagonal $BaBr_2$; the bar graph in figure 1(a) represents the corresponding powder diffraction data (PDF #45-1314) [4]. There is no phase transition from the hexagonal to orthorhombic phase $BaBr_2$ as was found in Eu-doped FBZ glass ceramics [5].

The XRD peaks are wider than the instrumental resolution of 0.085°, suggesting size-broadening effects. We estimate the particle sizes by using the Scherrer formula [6]

$$d = \frac{K\lambda}{(\Delta - 0.085°)\cos(\vartheta)} \quad (1)$$

with d the particle size, K the Scherrer constant (which is set to one in our analysis), λ the wavelength of the incident x-ray beam, 2ϑ the peak position of the reflection, and Δ the full width at half maximum of the reflection. We did not consider any stress or strain effects which may also lead to additional line broadening. The Scherrer formula is applied to the (111) reflection of hexagonal phase $BaBr_2$ at 28.0°; the line profile is fitted by a Lorentzian (figure 1(b)).

The particle sizes of the as-made sample and after thermal processing at 260 and 270 °C are between 15 and 30 nm;

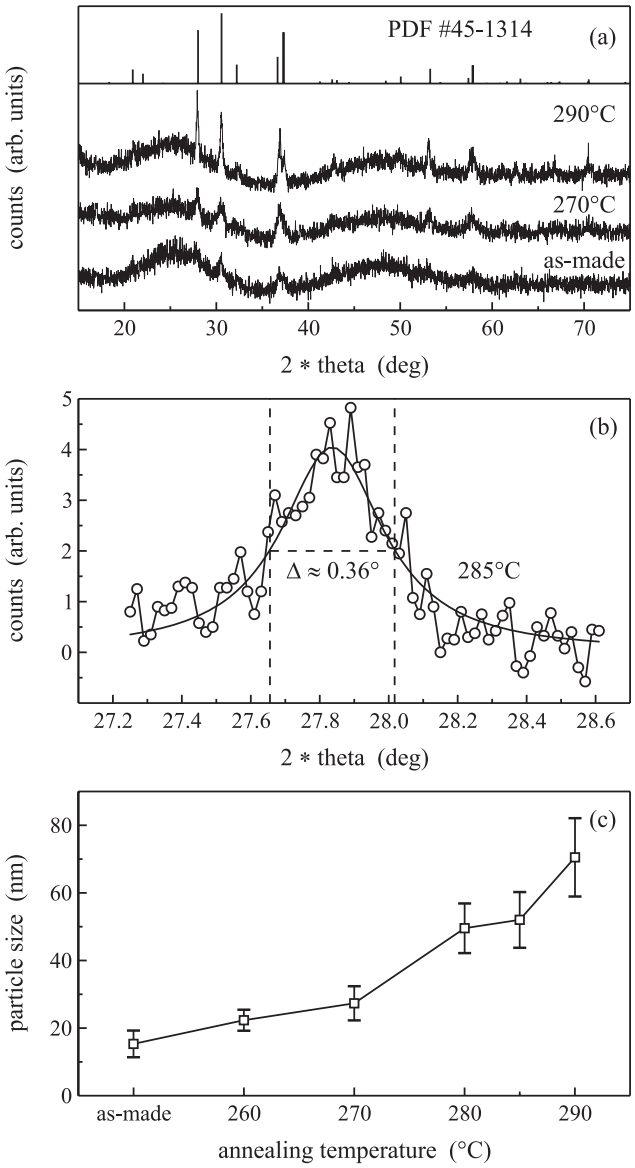

Figure 1. (a) XRD data for Sm^{2+}-doped FBZ glasses as-made and annealed for 20 min at 270 and 290 °C. The line pattern of hexagonal phase $BaBr_2$ (PDF #45-1314) is shown for comparison. (b) XRD peak used for the particle analysis of the 285 °C sample and the corresponding Lorentzian fitting curve. (c) Particle size versus annealing temperature. The line is a guide to the eye.

for annealing temperatures at 280 °C and above the particles grow from 50 nm to about 70 nm (figure 1(c)). Despite the poor signal-to-noise ratio of the XRD reflections, the Scherrer analysis provides a first estimate of the particle size; there is a trend to bigger particles for higher annealing temperatures. The particle growth proceeds from the precipitation of small hexagonal nanocrystals through Ostwald ripening: small particles will re-dissolve, and the larger ones will grow at the expense of the smaller ones.

3.2. Fluorescence spectroscopy

Samarium can enter the glass matrix either in its divalent form and/or as a trivalent ion. The fluorescence spectrum of FBZ

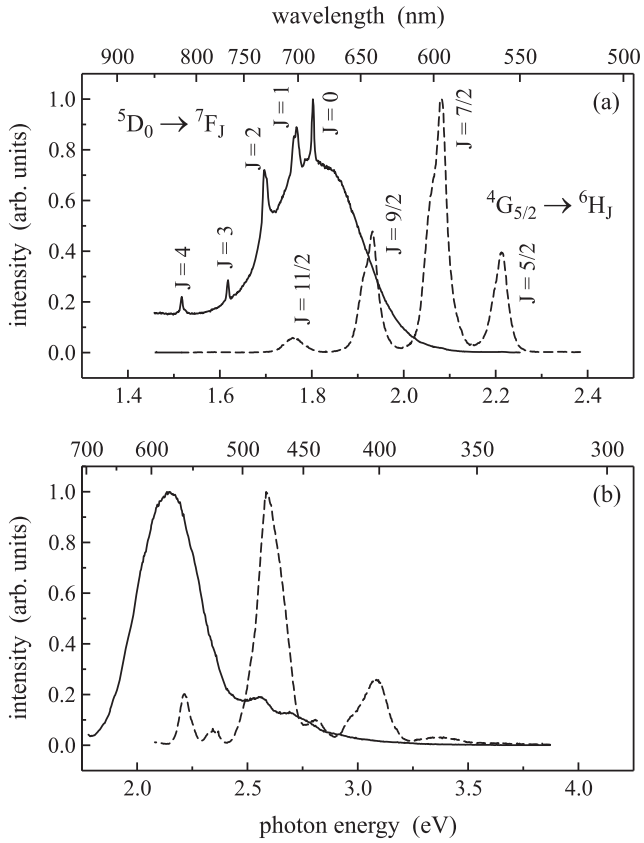

Figure 2. Normalized fluorescence spectra of FBZ glasses containing Sm^{2+} (solid curves) or Sm^{3+} (dashed curves). (a) Emission spectra excited at 590 nm (Sm^{2+}) and at 476 nm (Sm^{3+}), (b) excitation spectra detected at 730 nm (Sm^{2+}) and at 640 nm (Sm^{3+}). All spectra were recorded at room temperature.

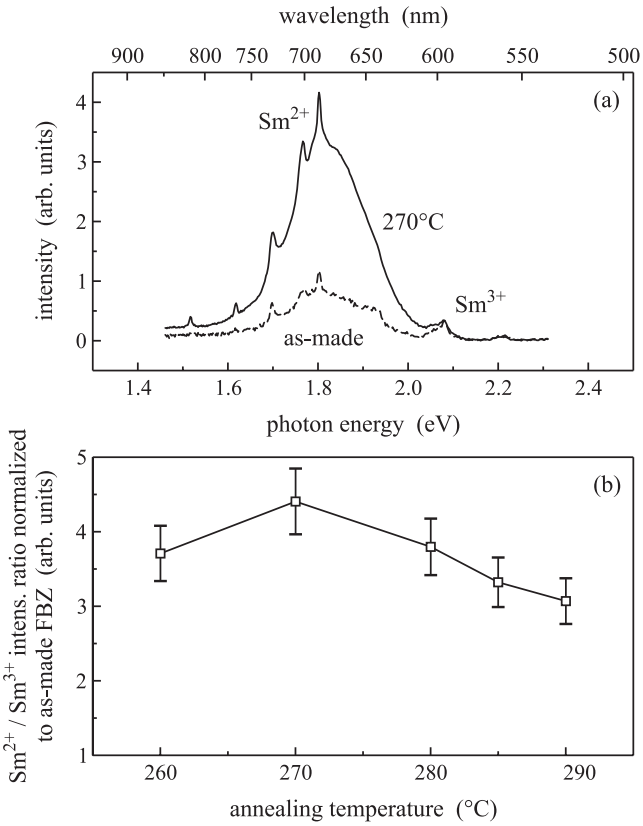

Figure 3. (a) Emission spectra of FBZ glasses containing both Sm^{2+} and Sm^{3+}, as-made and annealed for 20 min at 270 °C. (b) Sm^{2+}/Sm^{3+} fluorescence intensity ratio versus annealing temperature normalized to as-made FBZ. The line is a guide to the eye.

glass ceramics containing Sm^{2+} ions (figure 2(a), solid curve) shows relatively sharp lines of Sm^{2+} at 690, 700, 730, 765, and 815 nm which originate from $^5D_0 \rightarrow {}^7F_J$ ($J = 0, 1, 2, 3, 4$) transitions. In addition to the narrow line emissions, a broadband emission peaking at about 700 nm can be observed; the broadband emission can be attributed to a $4f^55d \rightarrow 4f^6$ transition [7]. The Sm^{2+} excitation spectrum is shown in figure 2(b), solid curve.

The Sm^{3+} emissions in FBZ (figure 2(a), dashed curve) are caused by transitions from the excited state $^4G_{5/2}$ to the ground state levels $^6H_{5/2}$ (560 nm), $^6H_{7/2}$ (595 nm), $^6H_{9/2}$ (640 nm), and $^6H_{11/2}$ (705 nm). The results agree with previous findings in Sm^{3+}-doped FZ fibers [8]. The corresponding excitation spectrum is depicted in figure 2(b), dashed curve.

Figure 3(a) shows the fluorescence spectra of FBZ glasses which contain Sm^{2+} and Sm^{3+} ions. Upon annealing the Sm^{2+} fluorescence intensity of the 270 °C annealed sample (solid curve) is increased by a factor of 4–5 with respect to the as-made sample (dashed curve); the Sm^{3+} intensity does not change upon annealing. The Sm^{2+}/Sm^{3+} ratio versus annealing temperature is plotted in figure 3(b); the Sm^{2+}/Sm^{3+} ratio is normalized to the value of the as-made sample.

3.3. Fluorescence lifetime

Figures 4(a) and (b) show the fluorescence decay curves for Sm^{2+} and Sm^{3+} in as-made FBZ and FBZ glass ceramics annealed for 20 min at different temperatures. The Sm^{2+} decay was recorded for the $^5D_0 \rightarrow {}^7F_0$ transition (690 nm) and the Sm^{3+} decay for the $^4G_{5/2} \rightarrow {}^6H_{7/2}$ transition (595 nm). The fluorescence lifetimes of the narrow line ($^5D_0 \rightarrow {}^7F_J$) and the broad band ($4f^55d \rightarrow 4f^6$) emissions of Sm^{2+} are identical within experimental error. Figure 4(c) shows that the Sm^{2+} fluorescence lifetime in FBZ glass ceramics increases upon annealing. The lifetime of Sm^{3+}, however, does not change upon thermal processing; it is (2.2 ± 0.2) ms for the as-made and all annealed samples.

4. Discussion

Both the fluorescence efficiency and lifetime of Sm^{2+} in FBZ glass ceramics can be significantly increased upon appropriate annealing. The investigation of samples here which contain Sm^{2+} and Sm^{3+} ions showed that the annealing affects the fluorescence properties of Sm^{2+} while those of Sm^{3+} remain unchanged.

The fact that the Sm^{2+} lifetime is increased, but the Sm^{3+} lifetime does not change within experimental error indicates that a part of the Sm^{2+} present in the glass matrix enters

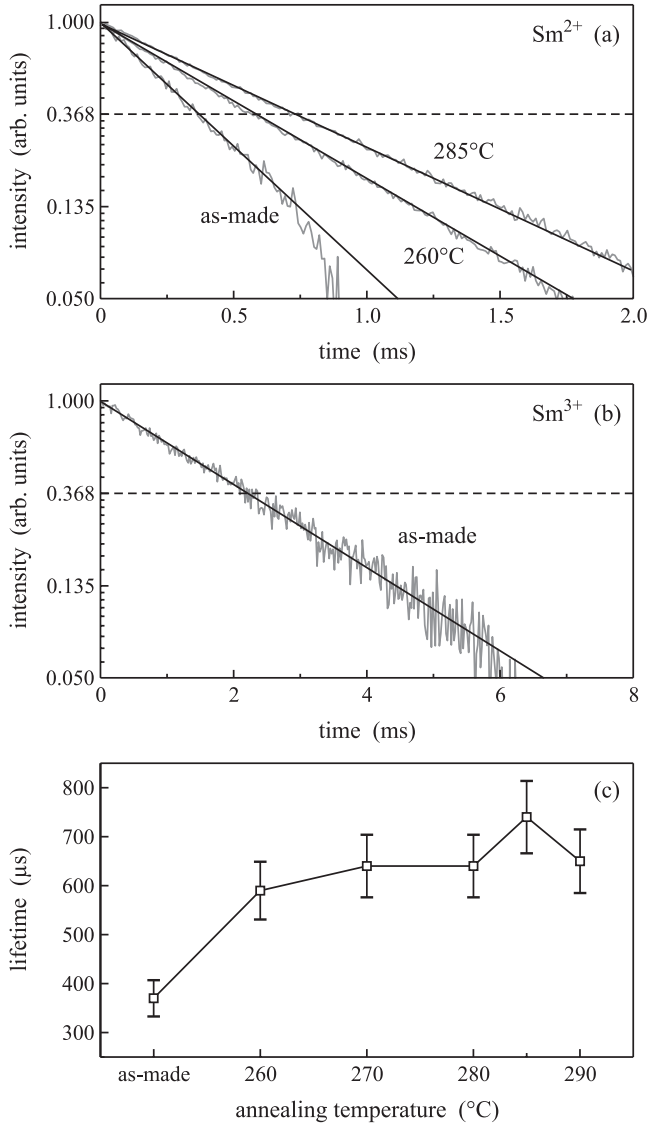

Figure 4. Decay of the Sm fluorescence in FBZ glasses. (a) The Sm^{2+} emission was detected at 690 nm ($^5D_0 \rightarrow {}^7F_0$). (b) The Sm^{3+} emission was detected at 595 nm ($^4G_{5/2} \rightarrow {}^6H_{7/2}$). (c) Decay time of the Sm^{2+} fluorescence in FBZ glass ceramics versus annealing temperature. The line is a guide to the eye. All measurements were carried out at room temperature; the fluorescence was excited at 590 nm for Sm^{2+} and at 476 nm for Sm^{3+}.

the $BaBr_2$ nanocrystals which are formed during thermal processing. Sm^{2+} probably substitutes for a barium ion on a regular lattice site while the incorporation of Sm^{3+} requires an additional charge compensation. The measured Sm^{2+} lifetime therefore has contributions from Sm^{2+} in the glass and from Sm^{2+} in the nanocrystals. Since the fluorescence lifetimes are increased upon annealing the phonon energies of the $BaBr_2$ nanocrystals are possibly smaller than those of the FZ base glass, i.e. the non-radiative losses are reduced, the overall measured lifetime is longer and thus the fluorescence is more efficient.

The above is, in principle, consistent with our observations. However, the fluorescence intensity versus annealing temperature plot (figure 3(c)) does not follow the trend given by the fluorescence lifetime versus annealing temperature graph (figure 4(c)): for annealing temperatures at 280 °C and above the fluorescence is slightly reduced with respect to the value for the 270 °C sample. We assume that for higher annealing temperatures light scattering effects are playing an increasingly important role. The $BaBr_2$ particles now have a size of larger than 50 nm, which may cause more light scattering and thus slightly reduced fluorescence intensities.

In analogy to our previous work on Eu-doped fluorobromo and fluorochlorozirconate glass ceramics [9, 10] we expect that the fluorescence efficiency, as well as the lifetime, depends significantly on the quantity of Sm^{2+} ions incorporated into the nanocrystals and how large the $BaBr_2$ nanocrystals are. The nominal samarium doping level for the glass is 1 molar% but the number of Sm^{2+} ions present in the nanocrystals is probably much smaller than that. Future work will be focused on optimizing the Sm^{2+} concentration in the nanocrystals.

Acknowledgments

This work was supported by the FhG Internal Programs under Grant No. Attract 692 034. Funding by the German Science Foundation (DFG project PAK88) and the Federal Ministry of Education and Research (BMBF) within FLUOPLEX under project number 13N8849 is gratefully acknowledged.

References

[1] Johnson J A, Schweizer S, Henke B, Chen G, Woodford J, Newman P J and MacFarlane D R 2006 *J. Appl. Phys.* **100** 034710
[2] Johnson J A, Schweizer S and Lubinsky A R 2007 *J. Am. Ceram. Soc.* **90** 693
[3] Aggarwal I D and Lu G (ed) 1991 *Fluoride Glass Fiber Optics* (New York: Academic)
[4] Liu G and Eick H A 1989 *J. Less-Common Met.* **149** 47
[5] Edgar A, Secu M, Williams G V M, Schweizer S and Spaeth J-M 2001 *J. Phys.: Condens. Matter* **13** 6259
[6] Scherrer P 1918 *Nachr. Ges. Wiss. Gött.* **2** 98
[7] Lauer H V Jr and Fong F V 1976 *J. Chem. Phys.* **65** 3108
[8] Saissy A, Azami N, Jones J and Maze G 1997 *Appl. Opt.* **36** 5931
[9] Secu M, Schweizer S, Spaeth J-M, Edgar A, Williams G V M and Rieser U 2003 *J. Phys.: Condens. Matter* **15** 1097–108
[10] Schweizer S, Hobbs L W, Secu M, Spaeth J-M, Edgar A, Williams G V M and Hamlin J 2005 *J. Appl. Phys.* **97** 083522